



## FRAGILITY EVALUATION OF RC BUILDING DESIGNED BY NEPAL BUILDING CODE CONSIDERING DEFORMATION CAPACITY

P. Adhikari<sup>(1)</sup>, A. Varma<sup>(2)</sup>, T. Azuhata<sup>(3)</sup>

<sup>(1)</sup> Engineer, Department of Urban Development and Building Construction (DUDBC), [praveenadhikari76@gmail.com](mailto:praveenadhikari76@gmail.com)

<sup>(2)</sup> Engineer, Department of Roads (DOR), [akv.osm@gmail.com](mailto:akv.osm@gmail.com)

<sup>(3)</sup> Research Engineer, International Institute of Seismology and Earthquake Engineering (IISEE), Building Research Institute (BRI), [azuhata@kenken.go.jp](mailto:azuhata@kenken.go.jp)

### Abstract

This research focuses on the fragility evaluation of a reinforced concrete (RC) building to investigate the intensity of earthquakes that the buildings designed by the current building codes in Nepal can resist. A published hazard map for Nepal presents the peak ground acceleration (PGA) by earthquakes of which return period is 500 years ranges 0.1 to 0.4 G. A seven-story office building was selected for the analysis. The initial non-linear static push-over analyses showed that shear failures might occur in this building, and thus the material specification was revised to achieve the required performance level by avoiding shear failures. Later the fragility analysis of this revised model was proceeded, comparing with that of the original one.

The probability of building collapse was determined by incremental dynamic analysis (IDA) with the scaled 40 different ground motions. For the original building model, the probability of the collapse was 30% to the PGA of 0.4 G. Contrary, that of the revised model decreased to about 5%. This result shows that the failure mode affects the fragility of buildings significantly.

The results of this study indicate that RC frame structures designed by NBC can perform satisfactorily with a design that guarantees ductility of the structure appropriately.

Keywords: *Fragility, Failure mode, Shear design, deformation capacity, Peak ground acceleration*

### 1. Introduction

Nepal lies on the Main Himalayan Thrust fault line that divides the Indian and Eurasian tectonic plates. The movement of the Indian Plate towards north collided with the Eurasian Plate. The collision between these two plates is still continuous at an average rate of about  $21 \pm 1.5$  mm per year slip along the plate boundary [1]. Due to inter-plate crustal shortening activity, the probability of the occurrence of an earthquake is very high in the Himalaya Range. As per the 2019 status report published by UNDRR (UN Office for Disaster Risk Reduction), Nepal stands at the top 11th rank in earthquake risk. The recent big earthquake occurred in Nepal was the Gorkha Earthquake in 2015 (Mw 7.8) resulted in huge losses of lives and physical infrastructures (8,891 people died, 610,702 houses fully destroyed, and 302,774 houses partially destroyed). To overcome these types of earthquake fatalities, we need earthquake-resistant resilient structures based on seismic performance design. The purpose of this study is to evaluate the seismic performance of a target RC structure building designed by Nepal Building Code (NBC105:1994, Seismic Design of Buildings in Nepal and NBC 110:1994, Plain and Reinforced Concrete) and to know the intensity of an earthquake the buildings can sustain.



In this research study, only the bare frame RC structure in the building is considered. This is the major limitation of the study. The confined masonry brick infill wall is neglected in the study because RC members are given to the priority in the design. The scope of this study is to investigate the reason why some RC members in the target building generated the shear failure and propose the appropriate methods to change the failure mode. Furthermore, we discuss how the fragility is mitigated by changing the failure mode.

## 2. Outline of Nepal National Building Code

### 2.1 Seismic action and design spectrum

The current Nepal National Building Code (NBC) comprises 23 different volumes which are categorized in four parts based on requirements and professionalism.

For seismic action, we estimate the horizontal seismic base shear force at first and distribute this base shear proportionately to each level or story of the building to obtain the horizontal seismic force. In NBC 105:1994 (Seismic Design of Buildings in Nepal), there is a provision of the computation of both horizontal seismic base shear force and horizontal seismic force at each level.

The horizontal seismic base shear force  $V$  in the direction under consideration is calculated by Eq. (1) (*cf.* NBC 105, cl. 8.1.1, cl. 10.1.1, and cl. 10.2.1):

$$V = C_d W_t = (CZIK)W_t \quad (1)$$

where,

$C_d$ : Design horizontal seismic force coefficient,

$C$ : Basic seismic coefficient for the fundamental translational period  $T$  in the direction under consideration (obtained from basic response spectrum, Fig.1),

$Z$ : Seismic zoning factor (obtained from seismic zoning map, Fig.2),

$I$ : Importance factor (1.0 ~ 2.0, as per Table 0.1 of NBC 105; For functional RC building, it is considered as 1.5),

$K$ : Structural performance factor, which is the function of minimum ductile detailing requirement (1.0 ~ 4.0, as per NBC 105; higher 'K' values correspond to less ductility and vice versa.), and

$W_t$ : Total gravity load above the level of lateral restraint.

The horizontal seismic force at each level  $i$  shall be calculated by Eq. (2)

$$F_i = V W_i h_i / \sum (W_i h_i) \quad (2)$$

where,  $W_i$  is the weight of the level  $i$  and  $h_i$  is the height to there from the lateral restraint level.

The fundamental period of the building structure in the direction under consideration is calculated by Eq. (3), Eq. (4), and Eq. (5) respectively (*cf.* NBC 105, Cl. 7.3):

a) For steel framed structures with no rigid elements limiting the deflection:

$$T_1 = 0.085 H^{3/4} \quad (3)$$

b) For concrete framed structures with no rigid elements limiting the deflection:

$$T_1 = 0.06 H^{3/4} \quad (4)$$

c) For other structures:

$$T_1 = (0.09 H) / \sqrt{(D')} \quad (5)$$

where,  $H$  is the height of the structure above the level of lateral restraint, and  $D'$  is the overall length of building in the direction under consideration.

The basic seismic coefficient  $C$  is obtained from the basic response spectra shown in Fig. 1. In the basic response spectra, there are three types of site subsoil, those are Type I, Type II, and Type III which represent the rock or stiff or hard soil sites, medium soil sites, and soft soil sites respectively.

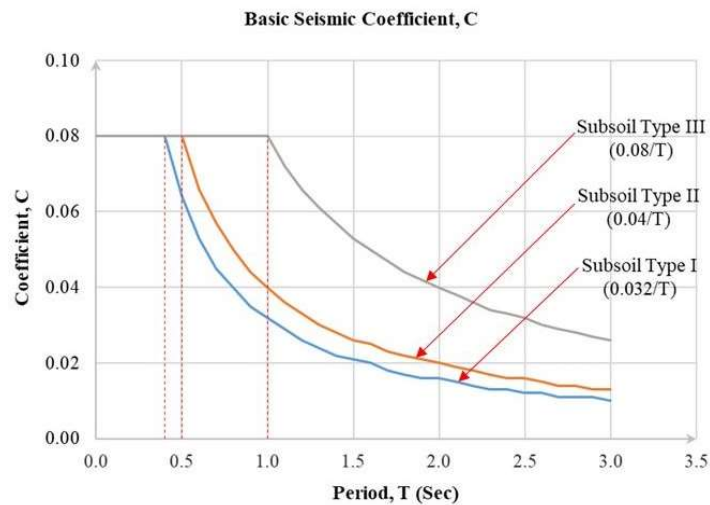


Fig. 1 – Basic response spectra (*cf.* NBC 105:1994 Seismic Design of Buildings in Nepal, cl. 8.1.4).

The seismic zoning factor  $Z$  for the construction location shall be obtained from Fig. 2. The Number shown in solid contour line indicates the coefficient of zoning factor. The zone coefficient  $Z < 0.8$  indicates the minor damage risk, zone coefficient  $0.8 \geq Z < 1.0$  indicates the moderate damage risk, and  $Z \geq 1.0$  indicates the widespread collapse and heavy damage.

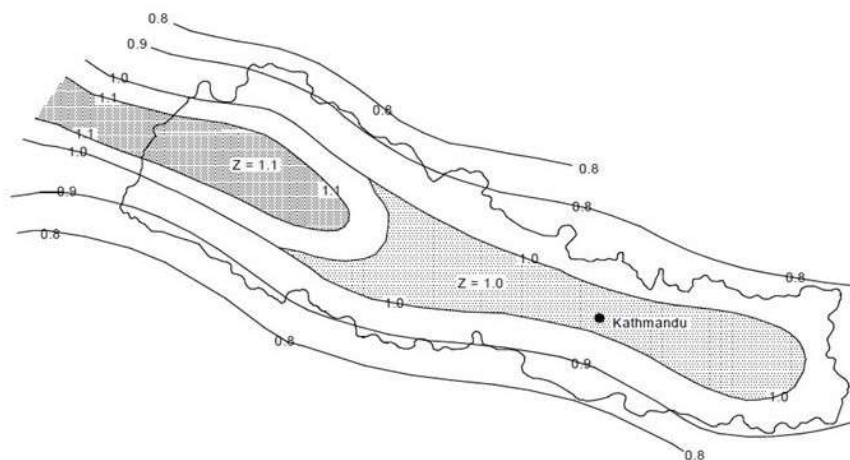


Fig. 2 – Seismic zoning factor,  $Z$  (*cf.* NBC 105:1994 Seismic Design of Buildings in Nepal, cl. 8.1.6).

## 2.2 Reinforced concrete code of Nepal

The reinforced concrete code of Nepal has been regulated by "NBC 110:1994 Plain and Reinforced Concrete." NBC 110 refers to the Indian Code "IS 456: 2000 Plain Concrete and Reinforced Concrete – Code of Practice." However, it has been modified to meet the conditions in Nepal and to be consistent with Nepal Standard, that is, NBC 105. For the design details of RC structures, "IS 13920: 2016 Ductile Design and Detailing of Reinforced Concrete Structures Subjected to Seismic Forces – Code of Practice" is also applied.

## 3. Methodology

### 3.1 Target building structure



In this study, a moment-resisting framed RC structure with 7 stories in the medium soil site condition is selected as the target structure. Fig.3 shows the elevations of it. The dimension of the structure is 27.94 m x 17.33 m with the height of 23.1 m. The column is 600 mm x 600 mm. The compressive strength of concrete of 20 N/mm<sup>2</sup> and tensile yield strength of steel rebar of 500 N/mm<sup>2</sup> is used in the structure.



Fig. 3 – Elevations of the target building (west and east).

The analytical model is constructed with the aid of the STERA 3D, Version 10.1 [2], which is shown in Fig. 4. The only bare frame structure is considered for response analyses. The flexibilities of footing beams and soil springs are neglected. Thus, the bases of columns on the ground floor are regarded as the fixed base.

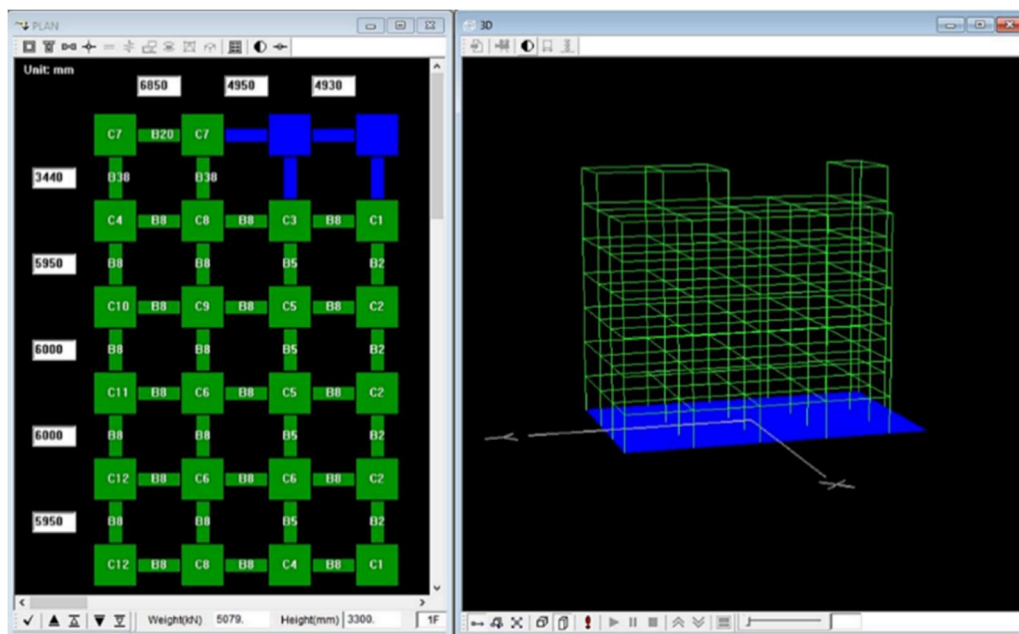


Fig. 4 – Analytical model of the target building by the STERA 3D computer program.

### 3.2 Analysis procedure

The research procedure for this study follows mainly three steps. Those are:



- Step 1: Determination of the limit state of the building by non-linear static pushover analysis,  
 Step 2: Execution of incremental dynamic analysis (IDA) [3], and  
 Step 3: Consideration on the fragility evaluation results.

For the IDA, we use a set of 40 ground motion data which were recorded in various earthquakes in California. These data are attained from the web-based PEER ground motion database [4] and the Center for Engineering Strong Motion Data (CESMD) [5]. The site condition of all ground motions is Type D of NEHRP (National Earthquake Hazards Reduction Program). The earthquake magnitude ranges from 6.5 to 6.9 Mw, and the source-to-site distance ranges from 13 to 40 km. Each ground motions are systematically scaled by the peak ground acceleration PGA, which are changed from 0.1 g to 1.5 g in the process of IDA. Altogether, 600 (40 x 15) numbers of the scaled earthquake are applied for the IDA. The acceleration response spectra of the 40 ground motions, of which PGA is scaled to 0.4 G, are shown in Fig. 5.

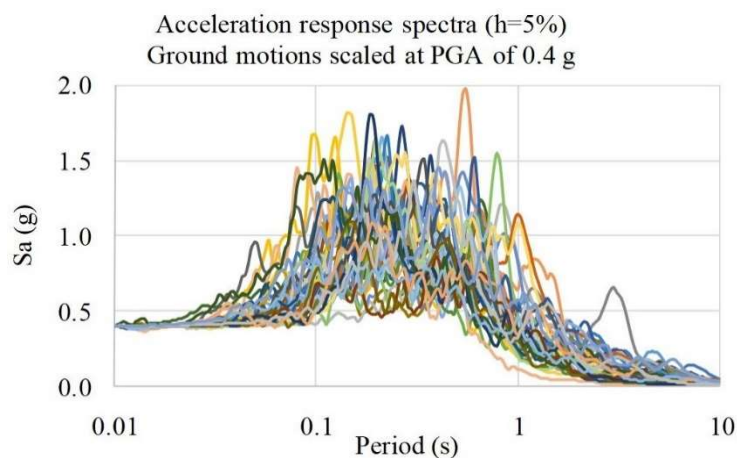


Fig. 5 – Acceleration response spectra of ground motions used for dynamic response analyses.

## 4. RESULTS AND DISCUSSION

### 4.1 Results for the original target building structure

The capacity curves of the target building are determined by non-linear static pushover analysis as shown in fig. 6. According to these capacity curves, we can judge that seismic capacity in x-direction is less than that of y-direction.

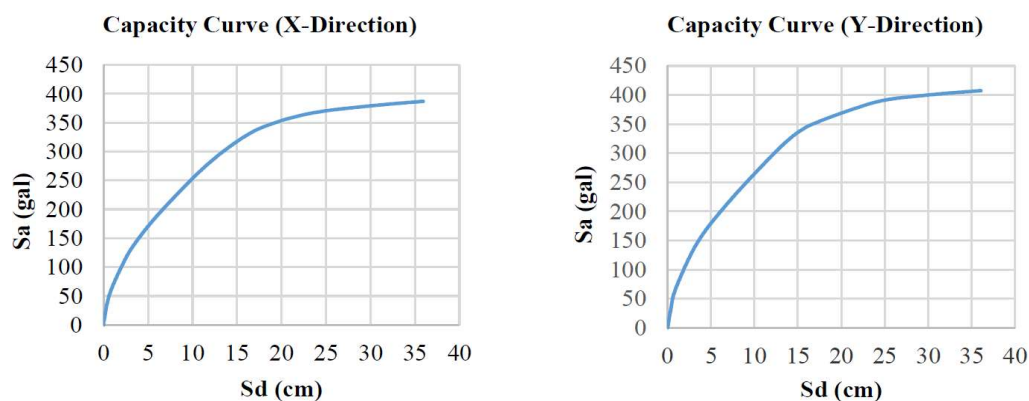


Fig. 6 – Capacity curve of the target building.



Fig.7 shows the drift-shear relation in the weaker direction. Each colored line indicates the drift-shear relation of the floors. From the push-over analysis, the first shear failure occurred at first floor in x-direction resulted in inter-story drift ratio of 0.011 ( $\approx 1/90$ ). Thus, the limit drift angle of the first floor is estimated to be  $1/90$ . The dashed red line indicates the drift-shear relation in each floor at this step. In Fig. 8, we can see this column which undergoes share failure firstly. The cause of this shear failure occurrence will be analyzed later.

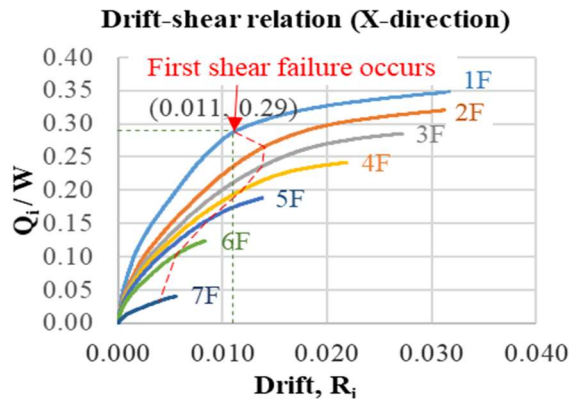


Fig. 7 – Drift-shear relation in x-direction.

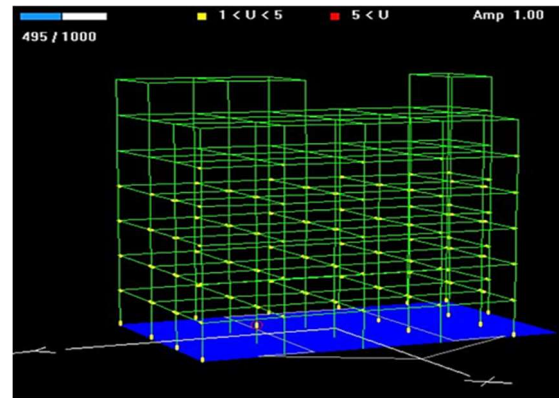


Fig. 8 – Failure mode.

Fig. 9 shows the results of the IDA. The maximum values of inter-story drift ratio for every earthquake ground motion are shown in this figure. Based on these analysis results, we derive the probability of collapse of the structure by using Eq. (6) for each PGA. And we consequently draw the fragility curve, as shown in Fig.10.

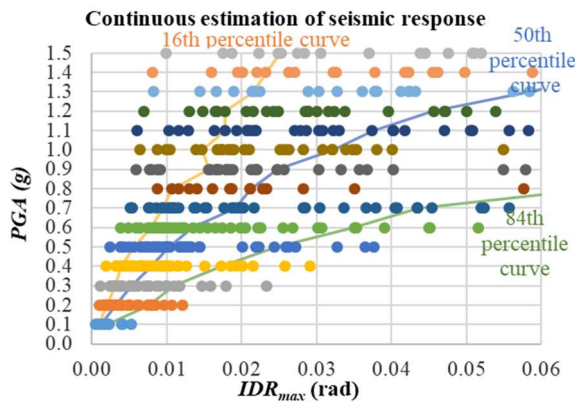


Fig. 9 – Statistics of seismic responses by IDA.

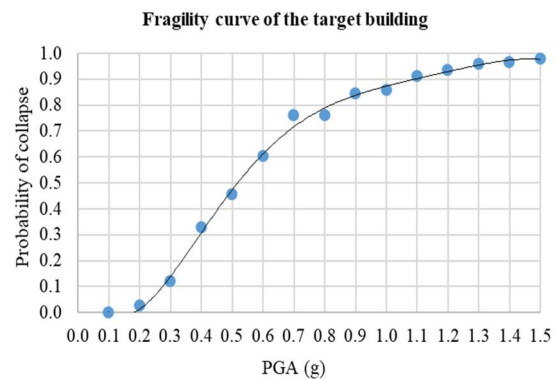


Fig. 10 – Fragility curve of the original model.

$$P[IDR_{\max} > IDR] = 1 - P[IDR_{\max} \leq IDR]$$

$$= 1 - \phi\left(\frac{\ln(x) - \ln(\mu)}{\delta}\right) \quad (6)$$

where,

$\phi$ : Normal cumulative distribution function,

$x$ : Limit state of the target structure, i.e.  $IDR$ ,

$\mu$ : Mean of the statistical data, evaluated by 50th percentile data, and



$\delta$ : Standard deviation of the statistical data, which is the equivalent dispersion of the 16th percentile and 84th percentile data of  $IDR_{max}$  in the normal distribution, computed by Eq. (7).

$$\delta = \frac{\ln(IDR_{max}[84\%]) - \ln(IDR_{max}[16\%])}{2} \quad (7)$$

where,  $IDR_{max}[84\%]$  is the 84th percentile and  $IDR_{max}[16\%]$  is the 16th percentile statistics data of the maximum inert-story drift ratio for specified scaled ground intensities.

The collapse probability becomes higher as PGA increase. According to the seismic hazard map of Nepal [6], the maximum PGA by earthquakes of which return period is 500 years is around 0.4 G. Fig. 10 indicates that the collapse probability for the PGA of 0.4G is 30%.

#### 4.2 Consideration on failure mechanism

Fig. 11 shows the cross-section of the column which yields in the shear failure mode firstly. Also, this figure shows the cross-section of the beams which are connected to this column in the x-direction. We can see this column undergoing the shear failure in Fig. 8, too. Fig. 12 shows the three concepts to determine the shear design force to ensure the bending failure mode to the column on the ground floor. According to each concept, the shear design force  $Q_{ms}$  is calculated as follows.

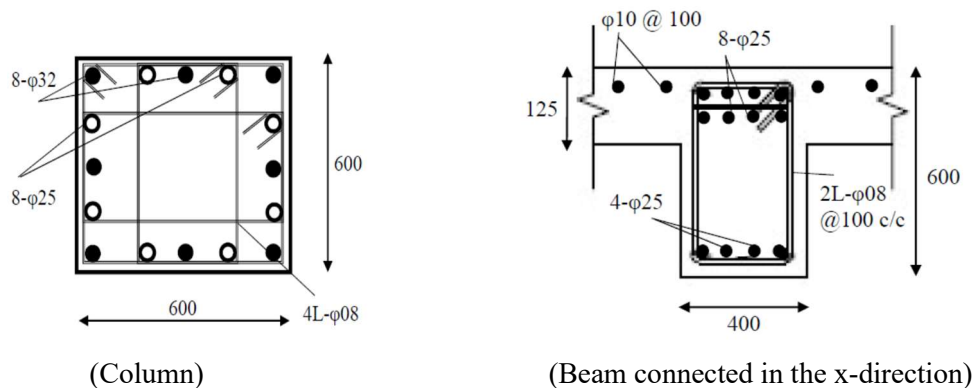


Fig. 11 – Cross-section of column which yields in the shear failure mode and beam connected to it.

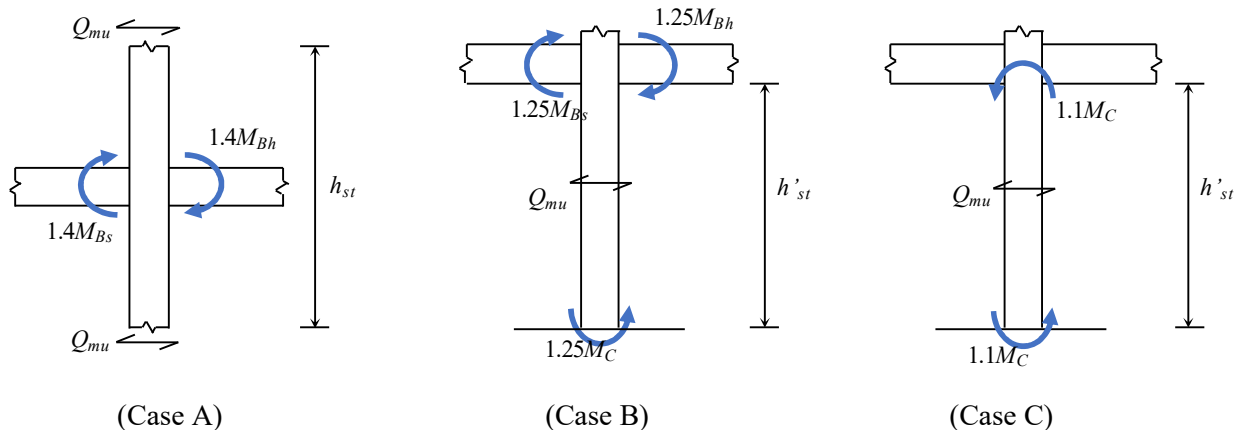


Fig. 12 – Concepts to determine shear design force.



$$\text{(Case A)} \quad Q_{mu} = 1.4 \frac{M_{Bs} + M_{Bh}}{h_{st}} \quad (8)$$

$$\text{(Case B)} \quad Q_{mu} = \frac{0.625(M_{Bs} + M_{Bh}) + 1.25M_C}{h'_{st}} \quad (9)$$

$$\text{(Case C)} \quad Q_{mu} = \frac{2.2M_C}{h'_{st}} \quad (10)$$

The concept of Case A is quoted from IS 13920. Since we assume the column bases are fixed to the rigid foundation neglecting flexibilities of footing beams in this study, this concept may be inadequate for setting the shear design force. The case B and C are based on the Japanese seismic code [7]. Since the target building is the weak beam-strong column system, the application of case B is appropriate.

The possible failure mode can be predicted by comparing the design shear force with the shear strength of the column. Table 1 shows the calculation results of the design shear forces  $Q_{mu}$  and the shear strength  $Q_{su}$ . We calculate the moment bending strengths of the column and the beam,  $M_{Bs}$ ,  $M_{Bh}$  and  $M_C$  in Fig., by formulas generally accepted in the seismic code of Japan [7]. These calculated values are not significantly different from the corresponding values calculated by the formulas accepted in Nepal. On the other hand, regarding the shear strength, we recognized a tendency that the values calculated by the Japanese formula (Arakawa's formula) are smaller than that based on the Nepalese seismic code (IS456). Thus, Table 1 shows the shear strengths calculated by both Japanese and Nepalese methods.

Table 1 – Comparison of shear strength  $Q_{su}$  with shear design force  $Q_{mu}$ .

	$Q_{mu}$ (kN)	$Q_{su}$ (kN)	
		Arakawa's fml	IS456
Case A	644.37	712.87	802.26
Case B	936.80		
Case C	1029.97		

Table 1 shows that except for Case A, the shear strengths are below the shear design force. This result means that shear failure will occur in the column. Also, it is consistent with the pushover analysis result by the STERA.

To avoid the shear failure of each member, we attempt to modify the target building model by adopting the following measures. Also, we evaluate the fragility of the revised model to investigate the effect of ensuring the bending failure mode.

- 1) Reducing the yield strength of reinforcement from 500 to 415 N/mm<sup>2</sup>.
- 2) Increasing the size of shear reinforcement (12 mm and 10 mm for column and beam respectively).
- 3) Providing additional shear reinforcement in the column in terms of legs, wherever necessary.

#### 4.3 Results of revised building model structure

The seismic performance of the revised model is analyzed in the same way for the original model. First, push-over analyses were executed. According to these results, no shear failure was observed in the revised model. The x-direction was weaker, and in this direction, the largest story drift occurred in the second story as shown in Fig. 13. Fig. 14 shows the mechanism in the x-direction obtained by the computer software, STERA 3D. The RC members were undergoing only a bending failure.

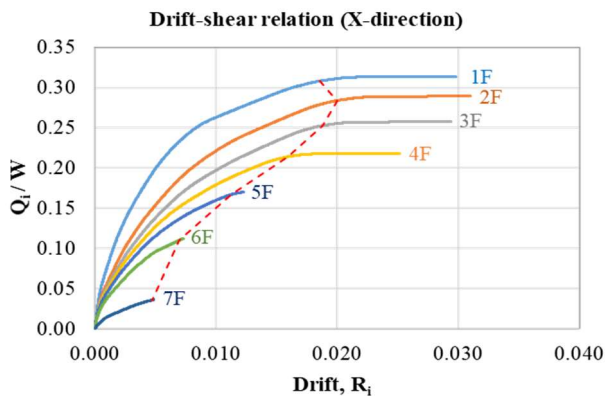


Fig. 13 – Drift-shear relation in the x-direction of the revised model.

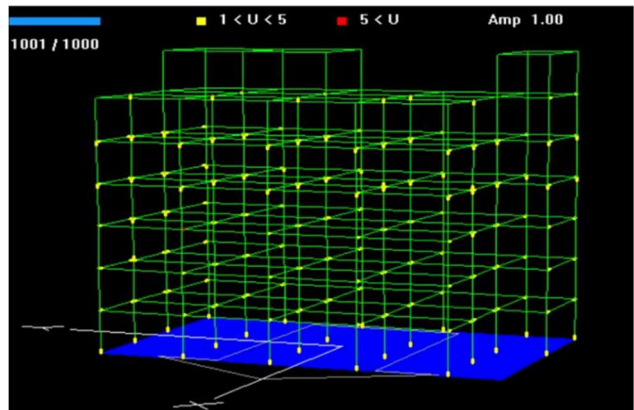


Fig. 14 – Failure mode in the revised model.

The maximum inter-story drift ratios for all scaled input ground motions were shown in Fig. 15. The probability of collapse was computed by Eq. (6). Consequently, the fragility curve for the revised model was derived, as shown in Fig. 16. In this analysis procedure, we assumed that the limit drift story angle is 1/30 based on empirical knowledge. The probability of collapse for the PGA of 0.4 G was reduced to 5 %.

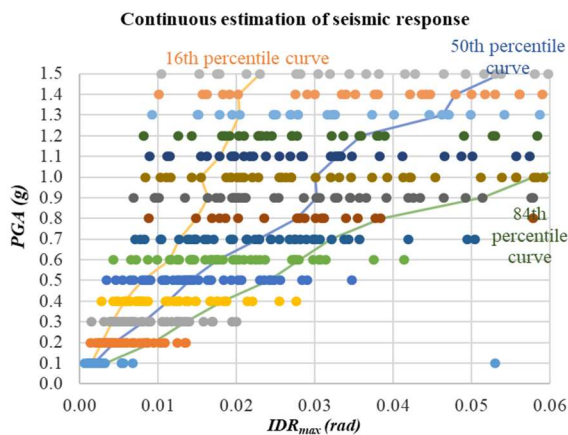


Fig.15 – Statistics of seismic responses by IDA of the revised model.

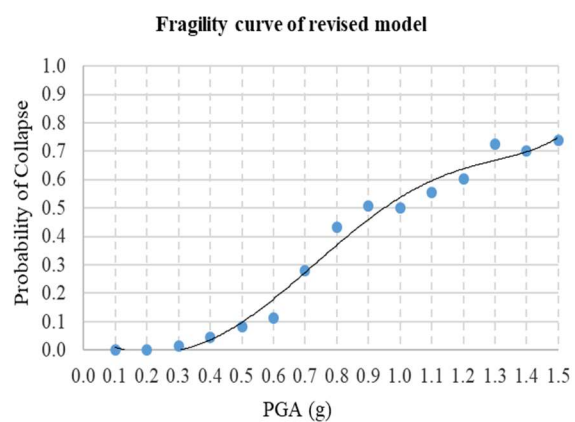


Fig. 16 – Fragility curve of the revised model.

#### 4.4 Comparison of fragility evaluation between original and revised model structure

Fig. 17 and Table 2 compare the fragility evaluation of the original model with that of revised model. For the revised model, which yields in the bending failure mode, the limit inter-story drift angle is assumed to be 1/50 or 1/30. The significant difference between them can be seen in Fig. 17 and Table 2. This result means that the seismic performance can be significantly improved by revising the failure mode shear to bending.

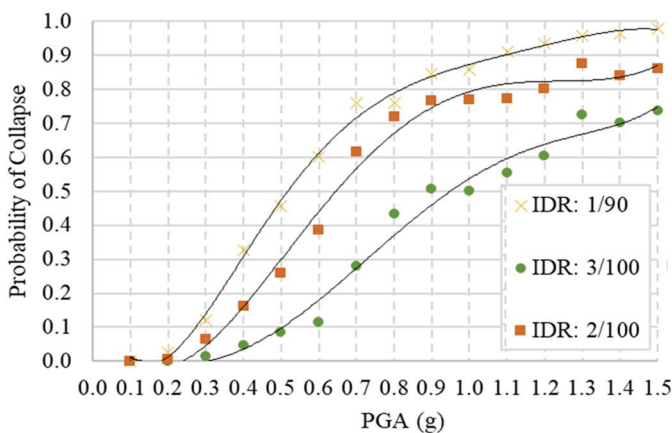


Fig. 17 – Comparison of Fragility curves.

Table 2 – Probability of collapse.

PGA (g)	P[ $IDR_{max} > IDR$ ]		
	IDR: 1/90	IDR: 2/100	IDR: 3/100
0.3	0.121	0.063	0.013
0.4	0.326	0.162	0.0459

Note)  $IDR$  of original model: 1/90  
 $IDR$  of revised model: 2/100 or 3/100

## 5. Conclusions

To investigate seismic performance of buildings designed by the current seismic building code of Nepal (NBC), we took up one office building as an example and evaluated the fragility of it. The analytical results and conclusions of this study are summarized as follows.

- 1) Before the incremental dynamic analyses (IDA) for the fragility evaluation, we carried out push-over analyses to grasp strength and deformation capacities of the target building. As a result, we found that the target building could cause shear failure. Thus, we made the revised model by revising some cross-sections of columns and beams of the original model to avoid shear failures.
- 2) We executed fragility evaluation by the IDA both to the original model and the revised model. The collapse probability when the PGA was 0.4G was about 30% for the original model but reduced to 5% for the revised model.
- 3) The above comparison result means that the seismic performance can be significantly improved by revising the failure mode shear to bending. For the example building shown in this study, such a change of the failure mode was relatively easy because it was possible only by revising the arrangement of bars, etc., without increasing the cross-sectional size.

The results of this study show that the RC frame structure designed by NBC can perform well, even in areas where large earthquakes are expected, with a design that guarantees ductility of the structure appropriately.

We adopted the assumption of the fixed base in this study. On the other hand, the designer may have considered the flexibility of the foundation beams in the actual design. In such a case, the failure mode of the original model could be bending failure. It is also conceivable that the masonry infill walls can work advantageously for seismic performance. With these favorable conditions, the collapse probability of the original model can be smaller than that shown in this study.

## 6. Acknowledgements

This study was conducted as a part of the 2019-2020 international training program for seismology and earthquake engineering implemented at the IISEE, BRI, supported by the Japan International Cooperation Agency (JICA). We would like to express our gratitude to all persons relating to this training program and our study.



## 7. References

- [1] Avouac, J.P., Meng, L., Wei, S., Wang, T., and Ampuero, J.P., 2015, Lower edge of locked Main Himalayan thrust unzipped by the 2015 Gorkha earthquake, *Nature Geoscience*, 8, 708–711.
- [2] Saito T (2019): Structural earthquake response analysis 3D, STERA 3D, <http://www.rc.ace.tut.ac.jp/saito/> (Only the current version, ver.10.3, is published.)
- [3] Vamvatsikos D, Cornell CA (2002): Incremental dynamic analysis. *Earthquake Engineering & Structural Dynamics*, 31 (3), 491-514.
- [4] Pacific Earthquake Engineering Research Center: PEER Ground Motion Database, <https://ngawest2.berkeley.edu/>.
- [5] Center for Engineering Strong Motion Data: CESMD – A Cooperative Effort, <https://strongmotioncenter.org/>.
- [6] Pandey MR, Chitrakar GR, Kafle B, Sapkota SN, Rajaure S, Gautam UP (2002): Seismic Hazard Map of Nepal, National Seismological Center, Ministry of Industry, Commerce and Geology, Nepal
- [7] Information Center of Building Administration, Japan Building Disaster Prevention Association (2016): Technical manual for standards of building structures, *Official Gazette Co-Operation of Japan*, Japan (In Japanese)